

1 Possible influence of atmospheric circulations on winter haze
2 pollution in Beijing-Tianjin-Hebei region, northern China

3
4 Ziyin Zhang^{1*}, Xiaoling Zhang¹, Daoyi Gong², Seong-Joong Kim³, Rui Mao²,
5 Xiujuan Zhao¹

6 ¹*Environmental Meteorology Forecast Center of Beijing-Tianjin-Hebei, Chinese
7 Meteorological Administration, Beijing 100089, China*

8 ²*State Key Laboratory of Earth Surface Processes and Resource Ecology, Beijing
9 Normal University, Beijing 100875, China*

10 ³*Korea Polar Research Institute, Incheon 406-840, Korea*

11
12 **Abstract:**

13 Using the daily records derived from the synoptic weather stations and the
14 NCEP/NCAR and ERA-Interim reanalysis data, the variability of the winter haze
15 pollutions (indicated by the mean visibility and number of hazy days) in Beijing-
16 Tianjin-Hebei (BTH) region during the period 1981 to 2015 and its relationship to the
17 atmospheric circulations in middle-high latitude were analyzed in this study. The winter
18 haze pollution in BTH had distinct inter-annual and inter-decadal variabilities without
19 a significant long-term trend. According to the spatial distribution of correlation
20 coefficients, six atmospheric circulation indices (I_1 to I_6) were defined from the key
21 areas in sea level pressure (SLP), zonal and meridional winds at 850 hPa (U850, V850),
22 geopotential height field at 500 hPa (H500), zonal wind at 200 hPa (U200), and air
23 temperature at 200 hPa (T200), respectively. All of the six indices have significant and
24 stable correlations with the winter visibility and number of hazy days in BTH. In the
25 raw (unfiltered) correlations, the correlation coefficients between the six indices and
26 the winter visibility (number of hazy days) varied from 0.57 (0.47) to 0.76 (0.6) with
27 an average of 0.65 (0.54); in the high-frequency (<10 yr) correlations, the coefficients
28 varied from 0.62 (0.58) to 0.8 (0.69) with an average of 0.69 (0.64). The six circulation
29 indices together can explain 77.7% (78.7%) and 61.7% (69.1%) variances of the winter
30 visibility and number of hazy days in the year-to-year (inter-annual) variability,
31 respectively. The increase of I_c (a comprehensive index derived from the six individual

* Correspondence to: Ziyin Zhang, Environmental Meteorology Forecast Center of Beijing-Tianjin-Hebei, Chinese Meteorological Administration, Beijing 100089, China.
E-mail: zzy_ahgeo@163.com

32 circulation indices) can cause a shallowing of the East Asian trough at the middle
33 troposphere and a weakening of the Siberian high pressure field at sea level, and then
34 accompanied by a reduction (increase) of horizontal advection and vertical convection
35 (relative humidity) in the lowest troposphere and a reduced boundary layer height in
36 BTH and its neighboring areas, which are favorable for the formation of haze pollutions
37 in BTH winter, and vice versa. The high level of the prediction statistics and the
38 reasonable mechanism suggested that the winter haze pollutions in BTH can be
39 forecasted or estimated credibly based on the optimized atmospheric circulation indices.
40 Thus it is helpful for government decision-making departments to take actions in
41 advance in dealing with probably severe haze pollutions in BTH indicated by the
42 atmospheric circulation conditions.

43 **Key word:** haze pollution, visibility, atmospheric circulation, Beijing-Tianjin-Hebei,

44

45 **1 Introduction**

46 Beijing-Tianjin-Hebei (BTH) region is located in northern China, with approximately
47 110 million residents and 216,000 km² in size. As the rapid progress of urbanization
48 and industrial development over the past three decades, the BTH region has become
49 one of China's most economically developed regions and the third economic engine in
50 China. Recently, the Chinese government has been promoting the integration of the
51 three neighboring regions to optimize the industrial layout and improve the allocation
52 of resources. Undoubtedly, the BTH region is becoming more and more important in
53 China or even the world economy in the future. However, the rapid economic growth
54 and urbanization have increased the level of air pollution in recent decades ([Streets et al., 2007](#);
55 [Chan and Yao, 2008](#); [Wang et al., 2009](#); [Wang et al., 2010](#); [Gao et al., 2011](#)).
56 Most of eastern China has frequently suffered from severe haze or smog days in recent
57 years, especially in the BTH region. For example, the continuously haze pollutions in
58 January 2013 greatly threatened human health and traffic safety ([Kang et al., 2013](#);
59 [Wang et al., 2013](#)). Roughly speaking, the haze pollution can be attributed to two
60 aspects: pollutant emissions to the lower atmosphere from fossil fuel combustion or
61 construction and favorable meteorological conditions. Meteorological conditions are
62 controlling the occurrence of haze pollution ([Wu, 2012](#); [Zhang et al., 2013](#)).
63 Specifically, weather conditions play an essential role in the daily fluctuation of air
64 pollutant concentrations ([Zhang et al., 2015](#)).

65 At present, many studies have focused on the physical and chemical properties of

66 pollutants in Beijing and other cities (Feng et al., 2006; Yu et al., 2011; Xu et al., 2013;
67 Zhao et al., 2013). And also studies demonstrated the influence of weather conditions
68 or synoptic situations upon air pollutions (Zhao et al., 2009; Zhang et al., 2015). They
69 elucidated clearly the formation and chemical composition of air pollutants and the
70 dominant meteorological factors during heavy pollution in the BTH region. On the
71 other hand, some studies demonstrated that the haze pollution occurring in the BTH
72 region could be strongly affected by the local atmospheric circulations including sea-
73 land and mountain–valley breeze circulations and the planetary boundary layer height
74 (Lo et al., 2006; Liu et al., 2009; Chen et al., 2009; Miao et al., 2015). Recently, Wang
75 et al. (2015) suggested that the reduction of autumn Arctic sea ice leads to anomalous
76 atmospheric circulation changes which favor less cyclone activity and more stable
77 atmosphere and leading to more hazy days in eastern China. Moreover, Wang et al.
78 (2013) showed that east China suffered from severe haze pollutions in January 2013
79 may be due to a sudden stratospheric warming over the mid-high latitude of Northern
80 Hemisphere, which lead to an anomalous steady atmosphere dominated in northern
81 China. Thus, it is interesting to examine whether the winter haze pollution in BTH has
82 been influenced by other known or unknown atmospheric circulations or
83 teleconnections in the mid-high latitude of the Northern Hemisphere and whether there
84 are some potential circulations that can be used for the forecast or evaluation of the
85 winter haze pollution in BTH. To date, it is not clear about these questions, and a few
86 studies have been performed to explore these issues.

87 Owing to a lack of long-term instrumental records for air pollutant concentration,
88 the understanding of the evolution of air pollution and their relations to atmospheric
89 circulations is limited. In this paper, we intend to use the atmospheric visibility and the
90 number of hazy days derived from the synoptic meteorological stations to denote the
91 evolution of haze pollution in the BTH region since 1980s. Many studies demonstrated
92 that, in the absence of certain weather conditions (e.g., rain, fog, dust and snowstorm),
93 the visibility is an excellent indicator of air quality because its degradation results from
94 light scattering and absorption by atmospheric particles and gases that can originate
95 from natural or anthropogenic sources (Baumer et al., 2008; Chang et al., 2009;
96 Sabetghadam et al., 2012; Baddock et al., 2014), although visibility was influenced
97 comprehensively by airborne pollutants and meteorological parameters such as relative
98 humidity, wind speed, temperature, pressure and solar radiation (Wen and Yeh, 2010;
99 Deng et al., 2014; Zhang et al., 2015) .

100 The main purpose of this study is to examine the possible relations between the

101 atmospheric circulations and the winter haze pollution (the mean visibility and mean
 102 number of hazy days) over the BTH region and investigate the possible physical
 103 mechanism, which could be useful for a prediction of the winter haze pollution and
 104 could provide a scientific support to the government to take effective measures in
 105 advance to reduce or control the pollutant emission in case of an anomalous circulations
 106 leading to a serious haze pollution in the region. This paper is organized as follows.
 107 Section 2 describes the data and method used. Section 3 shows major results and
 108 discussions. Conclusion is summarized in section 4.

109 **2 Data and methods**

110 **2.1 Research area and station data**

111 The atmospheric visibility recorded at the 19 synoptic meteorological stations
 112 located in the research area from 1 January 1980 to 28 February 2015 were used (Figure
 113 1). The visibility by human observers is recorded by four times (02:00, 08:00, 14:00
 114 and 20:00, Beijing local time) or three times (08:00, 14:00 and 20:00, Beijing local time)
 115 per day. A good continuous monitoring operation was maintained throughout the entire
 116 period, with the missing data rates for the 19 stations varying from a minimum of 1.7%
 117 to a maximum of 2.1%, with a mean 1.9%. On the other hand, the distribution of the
 118 stations is relatively uniform, indicating that the mean visibility or hazy days is a good
 119 representative for the whole BTH region.

120 In the present study, the days with visibility ≤ 5 km and relative humidity $< 90\%$
 121 at 14:00PM (local time) were defined as hazy days, except the special weather
 122 phenomena occurred at this moment including rain, fog, dust and snow (Schichtel et al.,
 123 2010; Wu et al., 2014;). The mean number of hazy days (\overline{NHD}) of each winter in the
 124 BTH region can be calculated by:

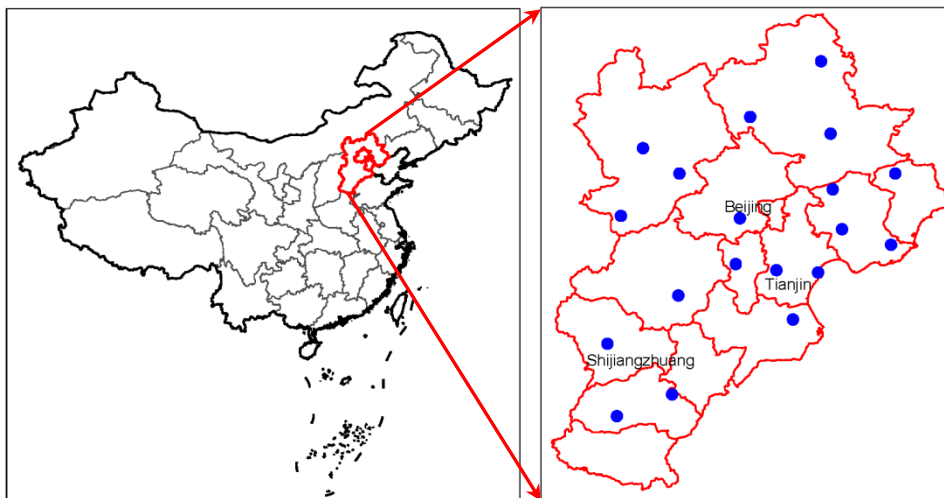
$$125 \quad \overline{NHD} = \frac{1}{n} \sum_{i=1}^n N_i \quad (1)$$

126 where n is the number of stations (here $n=19$), N denotes the number of hazy days
 127 in a station in each winter (December, January and February). The mean visibility (\overline{Vis})
 128 of each winter in the BTH region can be calculated by:

$$129 \quad \overline{Vis} = \frac{1}{n} \sum_{i=1}^n \left(\frac{1}{m} \sum_{j=1}^m V_{ij} \right) \quad (2)$$

130 where n is the number of stations (here $n=19$), m is the number of valid days in
 131 winter. It should be noted that the winter in 1981 consists of December 1980, January

132 and February 1981, and so on.



133

134 Figure 1 Research area and locations of the 19 synoptic meteorological stations

135 2.2 Reanalysis data

136 The global NCEP/NCAR reanalysis data of the monthly sea level pressure (SLP),
137 zonal and meridional winds at 850 hPa (U850, V850), geopotential height field at 500
138 hPa (H500), zonal wind at 200 hPa (U200) and air temperature at 200, 150, 100 and 70
139 hPa (T200, T150, T100, T70) with a $2.5^{\circ} \times 2.5^{\circ}$ spatial resolution from January 1980 to
140 February 2015 were used (Kalnay et al., 1996). Moreover, in order to obtain a higher
141 spatial resolution in the BTH region, the ERA-Interim reanalysis data of the monthly
142 relatively humidity (RH), vertical speed (W), zonal (U) and meridional (V) winds from
143 1000 to 500 hPa (16 pressure levels in total) and the boundary layer height (BLH) with
144 a $0.125^{\circ} \times 0.125^{\circ}$ spatial resolution confined to the area $33\text{-}45^{\circ}\text{N}$ and $110\text{-}122^{\circ}\text{E}$ were
145 also used (Dee et al., 2011).

146

147 2.3 Analysis method

148 For the statistical and atmospheric circulation analyses carried out in the study, the
149 common statistical methods such as the composite analyses and the least square
150 regression and the Pearson correlation analyses with a two-tailed Student's t-test were
151 applied in this research. A principal component analysis (PCA) was also used to extract
152 the principal mode of multiple time series. Moreover, in order to reduce the possible
153 effects of low-frequency variation or long-term trends and to examine whether or not
154 the correspondence between the two time series on inter-annual time-scale is stable, the
155 high-frequency ($< 10\text{yr}$) correlation of the high-pass filtered time series was also tested
156 for time series analyses (Gong and Luterbacher, 2008; Zhang et al., 2010).

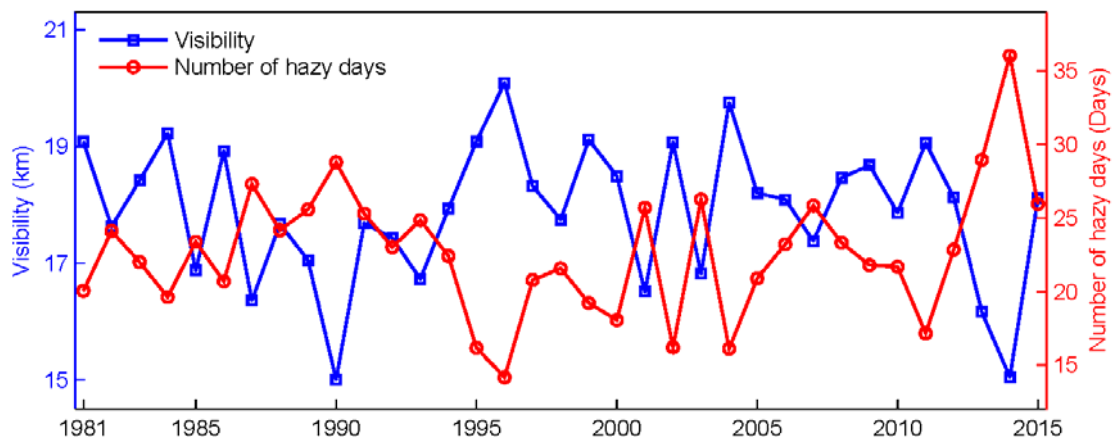
157

158 **3 Results and discussions**

159 **3.1 Evolution of the winter visibility and hazy days in the BTH region**

160 The regional mean visibility and number of hazy days in winter in BTH were
161 presented in Figure 2. As expected, the visibility was negatively correlated to the
162 number of hazy days with the raw and high-frequency (< 10yr) correlation coefficients
163 between them of -0.91 and -0.93, respectively. Both of them are significant at the 0.01
164 level ($p < 0.01$ for short). More hazy days generally denote lower mean visibility in
165 winter due to the light scattering and absorption effects of air pollutants (Baumer et al.,
166 2008; Sabetghadam et al., 2012). There are intense inter-annual fluctuations in both the
167 visibility and the number of hazy days over the entire period of 1981 to 2015. The
168 decadal fluctuations can be also distinguished for both the visibility and the number of
169 hazy days throughout the entire period. A significant reducing trend of visibility
170 ($p < 0.05$) and increasing trend of number of hazy days ($p < 0.01$) dominated in the 1980s.
171 And then, the visibility experienced an increasing trend in 1990s and a decreasing trend
172 since 2001, and the hazy days showed an anti-phase changes, but none of them are
173 statistically significant with exception of the number of hazy days trend in 1990s
174 ($p < 0.05$). The mean visibility maximum in 1990s reached to 18.3 km (larger than the
175 mean values of 17.9 km over the entire period); and the minimum number of hazy days
176 in 1990s reached to 20.6 days (less than the mean values of 22.7 days over the entire
177 period). However, the long-term trends of them are not statistically significant, although
178 a weak reducing and increasing trends can be founded in the curves of winter visibility
179 and number of hazy days, respectively.

180



181

182 Figure 2 Curves of the winter mean visibility and number of hazy days in BTH

183

184 **3.2 Relationship between haze pollution and atmospheric circulations**

185 We first examined the correlation coefficients between the visibility and number of
 186 hazy days and the most common atmospheric teleconnection or oscillation indices over
 187 the mid-high latitude of Northern hemisphere (see Table 1), which could affect the
 188 winter climate variability over China, such as the Arctic Oscillation (AO), the Northern
 189 Atlantic Oscillation (NAO), the Pacific/North American pattern (PNA), the Eurasian
 190 pattern (EU), the Western Pacific pattern (WP) and the Siberian High (SBH) (Wallace
 191 and Gutzler, 1981; Zhang et al., 2009; Gong and Ho, 2012). It can be seen that both of
 192 the raw ($r1$) and high-frequency ($r2$) correlations show that the visibility and number
 193 of hazy days are correlated weakly with the winter AO, NAO and PNA. However, the
 194 visibility is highly positively correlated with EU, WP and SBH; and the number of hazy
 195 days is highly negatively correlated with EU, WP and SBH, most of them are significant
 196 at the 0.01 or 0.05 level.

197

198

Table 1 Correlation coefficients of visibility and hazy days and circulation indices

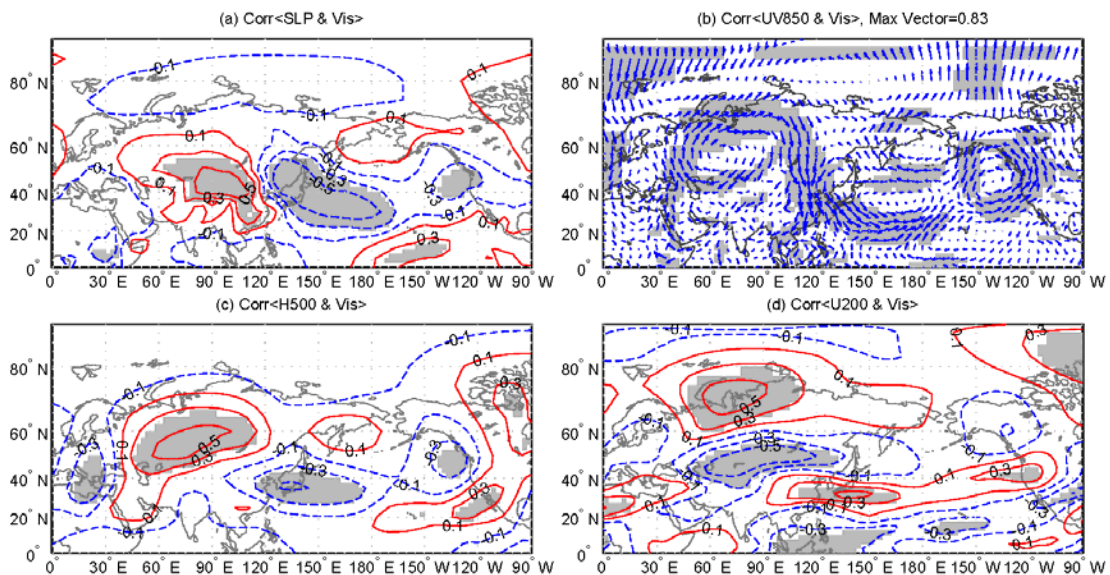
		AO	NAO	PNA	EU	WP	SBH
Visibility	$r1$	-0.11	0.00	0.16	0.61**	0.40*	0.39*
	$r2$	0.05	0.22	0.16	0.71**	0.37*	0.36*
Number of hazy days	$r1$	0.13	0.13	-0.10	-0.51**	-0.47**	-0.32
	$r2$	-0.01	-0.11	-0.10	-0.70**	-0.56**	-0.37*

199 ** Significant at the 0.01 level, * Significant at the 0.05 level. The $r1$ and $r2$ terms indicate the
 200 raw correlation and high-frequency (< 10yr) correlation, respectively.

201 Furthermore, the general characteristics of spatial distribution of the correlation
 202 coefficients between visibility and number of hazy days in BTH and the major
 203 meteorological fields from surface to tropopause in Northern Hemisphere including
 204 SLP, U850, V850, H500, U200, T200, T150 and T70 were also examined (Figure 3 and
 205 4). Owing to a generally anti-pattern for the number of hazy days, thus only the
 206 correlation maps with visibility were analyzed for simplicity. In SLP (Figure 3a), a
 207 positive correlation center dominated most of East Asian continent, while a negative
 208 correlation center dominated the area from northeast Asia to northwest Pacific,
 209 respectively. This spatial pattern may reflect the effects of land-sea thermal contrast on
 210 the lower troposphere condition over BTH region. The pressure increasing in East
 211 Asian continent and decreasing in area from northeast Asia to northwest Pacific suggest
 212 that they favor the visibility increase in the BTH region in winter, and vice versa. In
 213 UV850 (Figure 3b), an anomalously anti-cyclonic and northerly pattern are
 214 predominant most of Siberia and eastern China. This suggests that an anomalous

215 northerly advection from Siberian to eastern China improve the winter visibility in the
 216 BTH region. In H500 (Figure 3c), there exist a “-+” wave train pattern along the
 217 Eurasia-west Pacific in the mid-high latitude, extending from the central-eastern
 218 Europe through Siberia to north China-Korean peninsula-Japan-northwest Pacific
 219 Ocean, similar to the EU pattern (Wallace and Gutzler, 1981). This pattern implies that
 220 a deepening of East Asian trough and a weakening of blocking will favor the winter
 221 visibility increase in the BTH region. In U200 (Figure 3d), there also exist a wave train
 222 pattern from northwest Russia through Siberia to northwest Pacific Ocean. This pattern
 223 may imply that the south (north) of East Asian Jet stream strengthened (weakened)
 224 coincided with the anomalous ascending (sinking) motions occurred in the south (north)
 225 of the Jet stream entrance at the upper troposphere, which will lead to a strengthening
 226 northerly appeared in the lower troposphere. Hence it is not conducive to the
 227 accumulation of pollutants over BTH region in the winter.

228



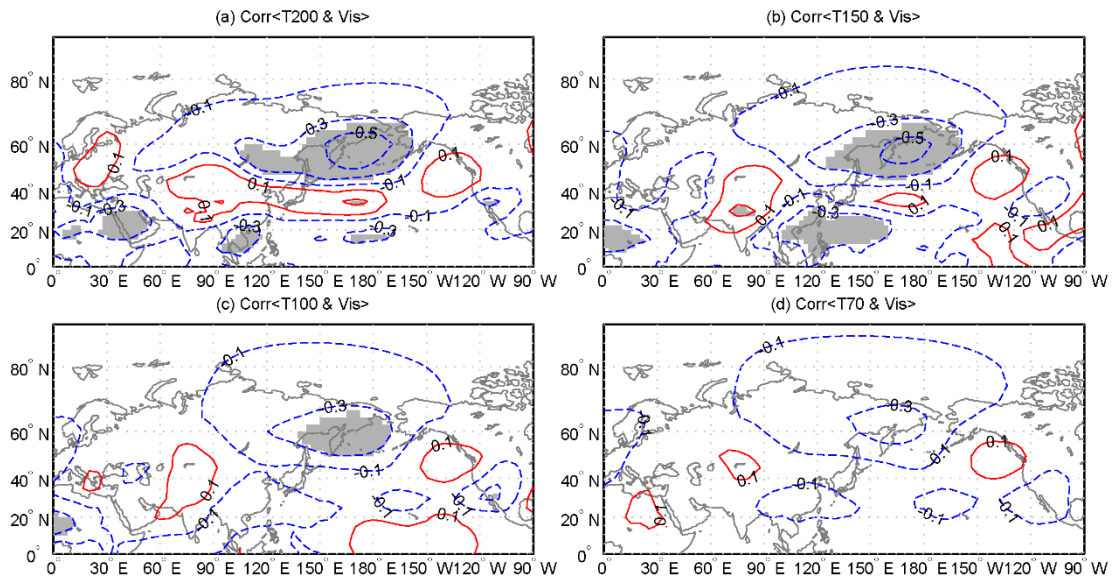
229

230 Figure 3, Spatial distribution of correlation coefficients between visibility and SLP (a), UV850
 231 (b), H500 (c) and U200 (d) (Area significant at the 0.05 level are shaded; either U850 or V850
 232 significant at the 0.05 level are shaded in b)

233

234 Besides the lower troposphere, previous studies suggested that the anomalous
 235 stratospheric warming over the Northern Hemisphere led to the severe haze pollutions
 236 in east China in January 2013 (Wang et al., 2013). Here, the spatial distribution of the
 237 correlation coefficients between visibility and the temperature from the upper
 238 troposphere to lower stratosphere at 200 hPa (T200), 150 hPa (T150), 100 hPa (T100)
 239 and 70 hPa (T70) were checked. Negative correlations are found from eastern Siberia

240 to the northern North Pacific including Alaska in T200, T150, T100 and T70,
 241 respectively (Figure 4), with the biggest correlation in T200 (Figure 4a). The
 242 significantly negative correlation suggest that the warming at 200 hPa over eastern
 243 Siberia to the northern North Pacific would indicate a decreasing of winter visibility,
 244 namely a worsening of haze pollutions in the BTH region.
 245



246
 247 Figure 4 Spatial distribution of correlation coefficients between visibility and T200 (a), T150 (b),
 248 T100 (c) and T70 (d) (Area significant at the 0.05 level are shaded)
 249

250 Based on the above analyses, we wonder whether the meteorological variables in
 251 the significant correlation areas can be used to predict or evaluate the variability of the
 252 winter visibility and haze pollutions in the BTH region. Thus, the six indices for
 253 atmospheric circulations or teleconnections were defined based on the key regions
 254 shown in the previous correlation maps as listed in Table 2. We computed the raw and
 255 high-frequency correlation coefficients of the winter visibility and number of hazy days
 256 in BTH and the six atmospheric circulation indices. All of the six indices (I_1 to I_6) show
 257 highly positive or negative correlations with the winter visibility and number of hazy
 258 days, with significance at the 0.01 level (Table3). Moreover, we note that most of the
 259 high-frequency correlations are larger than the raw correlations except the correlations
 260 between visibility and I_1 . This suggests that the links between the air quality in BTH
 261 and the circulations indices are very stable from year to year. The significantly positive
 262 or negative correlations should be a reflection of the physical response mechanisms
 263 between them, which will be discussed in the latter section.
 264

265

Table 2 List of the definition for the six circulation indices

Index	Variable	Expression
I ₁	SLP	SLP (38~50N, 84~108E) – SLP (36~52N, 126~150E; 24~40N, 150~184E)
I ₂	U _{850hPa}	U ₈₅₀ (55~75N, 40~110E) – U ₈₅₀ (40~50N, 45~75E)
I ₃	V _{850hPa}	V ₈₅₀ (32~64N, 104~120E)
I ₄	H _{500hPa}	H ₅₀₀ (46~64N, 50~92E) – H ₅₀₀ (28~44N, 16~28E; 28~42N, 120~156E)
I ₅	U _{200hPa}	U ₂₀₀ (42~52N, 60~110E) – U ₂₀₀ (64~76N, 50~96E; 28~36N, 120~152E)
I ₆	T _{200hPa}	T ₂₀₀ (46~66N, 146~196E)

266

267

268

Table 3 Correlation coefficients of visibility and number of hazy days and circulation indices

		I ₁	I ₂	I ₃	I ₄	I ₅	I ₆
Visibility	r1	0.73**	0.57**	-0.76**	0.62**	-0.59**	-0.61**
	r2	0.70**	0.68**	-0.80**	0.72**	-0.62**	-0.62**
Number of hazy days	r1	-0.60**	-0.47**	0.60**	-0.47**	0.52**	0.60**
	r2	-0.61**	-0.65**	0.69**	-0.67**	0.58**	0.64**

269

Same as Table 1

270

271 3.3 Predictions for visibility and number of hazy days based on the circulation 272 indices

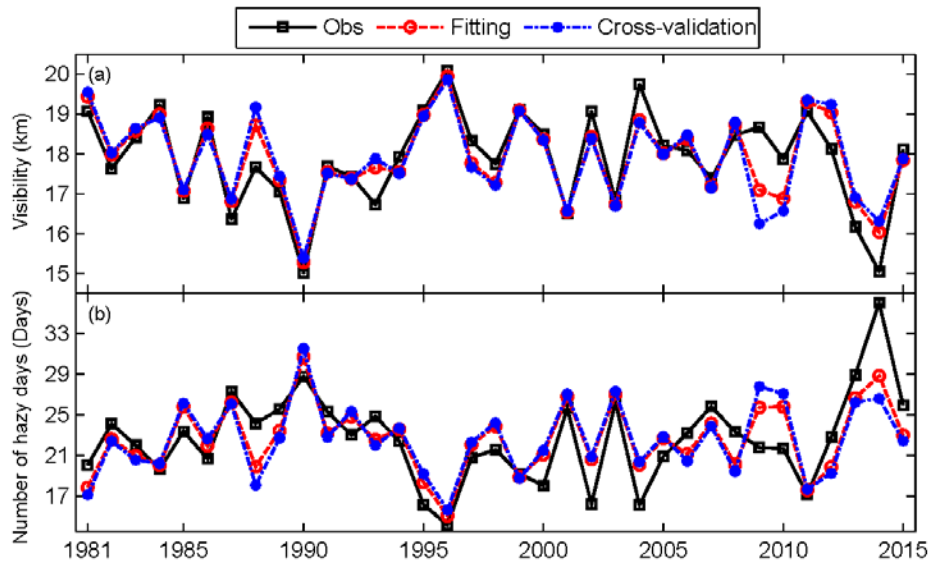
273 In order to assess the prediction capability of the six circulation indices for the
274 winter haze pollutions in BTH, the winter mean visibility and number of hazy days
275 were estimated by applying a multivariate regression method with the least square
276 estimate. The estimated curves by the fitting and the cross-validation with a leave-one-
277 out method were displayed in Figure 5. Intuitively, both of the fitting curves and the
278 cross-validation curves are fairly consistent with the observed winter mean visibility
279 and number of hazy days over the last three decades. The raw and high-frequency
280 correlation coefficients between the observed and the fitting visibility (number of hazy
281 days) are 0.88 (0.78) and 0.86 (0.77), respectively. All of them are significantly at 0.01
282 level. The six circulation indices together can explain 77.7% (78.7%) and 61.7%
283 (69.1%) variances of the winter visibility and number of hazy days over the BTH region
284 in the year to year (inter-annual) variability, respectively. A good fitting does not mean
285 that there must be stable relationships between the dependent variable and explanatory
286 variables. Thus we emphasized testing the stability of the statistic models by means of
287 the Leave-N-out cross-validations. The statistics for the cross-validation estimations

288 were listed in Table 4, including the explained variance (r^2), the standard error (SE),
289 and reduction of error (RE). Previous studies suggested that RE is an extremely rigorous
290 verification statistic because it has no lower bound, $RE > 0$ indicating the skillful
291 estimation, $RE > 0.2$ indicating the reliable estimation and $RE = 1.0$ indicating a perfect
292 estimation (Fritts, 1976; Gong and Luterbacher, 2008; Zhang et al., 2010).

293 The statistics for both the visibility and number of hazy days are generally stable
294 (no sharply increase or decrease) when N increased from 1 to 11 (more than 30% sample
295 removed in regression models), although the r^2 and RE (SE) slightly decreased
296 (increased) with the increasing of N. For the visibility, the r^2 varied from 52.5% to 62.7%
297 with an average of 57.6%, the SE varied from 0.74 to 0.84 with an average of 0.79, the
298 RE varied from 0.49 to 0.61 with an average of 0.55. For the number of hazy days, the
299 r^2 varied from 31.1% to 41.5% with an average of 35.2%, the SE varied from 3.37 to
300 3.66 with an average of 3.54, the RE varied from 0.23 to 0.38 with an average of 0.30.
301 The mildly changes of these statistics suggest that the statistic models between the given
302 atmospheric circulations and the haze pollution indicators are stably even in the case of
303 parts of sample missed. On the other hand, we noted the statistics for the visibility
304 estimations are generally better than that for the number of hazy days estimations in all
305 tests. However, the minimum values of r^2 and RE for the number of hazy days
306 estimations are still larger than 30% and 0.2, respectively. Based on these statistics, it
307 can be concluded that the predictions for the winter visibility and number of hazy days
308 in the BTH region based on the circulation indices are overall reliable during the entire
309 period, especially for the mean visibility. That is to say, the winter haze pollutions in
310 BTH can be evaluated or estimated well by the optimized atmospheric circulations.

311 The relatively larger errors for the estimated values referred to the observed
312 visibility and number of hazy days have been found since the winter in 2009 (Figure 5).
313 We re-computed all the statistics for the period 1981 to 2008, the results displayed that
314 all the values of r^2 and RE (SE) for visibility and number of hazy days predictions
315 increased (decreased) much more than the entire period (Table 4), suggesting that the
316 statistic estimation models are much more stable and reliable before 2009. Why did the
317 prediction efficiency of the statistic estimation models decrease relatively in the last
318 few years? It can be distinguished that the estimations for the winter mean visibility are
319 distinctly lower (higher) than the observed in the winters of 2009 and 2010 (2014), and
320 vice versa for the number of hazy days. We speculated that these phenomena can be
321 attributed partly to the fluctuations of pollutant emissions because the pollutant
322 emissions over northern China around 2008 were controlled strictly by the Chinese

323 government associated with the 2008 Olympic Games in Beijing (An et al., 2007;
 324 Zhang et al., 2010; Gao et al., 2011). The decrease of pollutant emissions led to the
 325 improvement of air quality (increasing visibility and decreasing hazy days) in 2009 and
 326 2010, although the atmospheric conditions remained the same and did not contributed
 327 to the spread and elimination of air pollutants. However, pollutant emissions especially
 328 in the areas of BTH rebounded after the Olympic Games, with the decrease in visibility
 329 and increase in hazy days in the BTH region around 2012 to 2014 to some extent (Zhang
 330 et al., 2015). Generally, the errors between the observed visibility (haze days) and the predicted
 331 could be attributed to the natural variability of atmospheric circulation and the changes of pollutant
 332 emissions. However, the contribution rates of each factor are not clear now, thus further studies will
 333 be necessary to unravel these issues.



334
 335 Figure 5 Curves of the observed and the predicted winter visibility (a) and number of hazy days
 336 (b) in the BTH region since 1981
 337

338 Table 4 List of the statistics for the Leave-N-out cross-validation estimations

N	Period covering	Visibility			Number of hazy days		
		r^2 (%)	SE	RE	r^2 (%)	SE	RE
1	1981-2015	62.7	0.74	0.61	41.5	3.37	0.38
	1981-2008	87.1	0.42	0.87	53.9	2.56	0.52
3	1981-2015	56.8	0.80	0.54	34.3	3.57	0.28
	1981-2008	86.8	0.42	0.87	52.6	2.59	0.51
5	1981-2015	59.2	0.78	0.57	35.3	3.54	0.30
	1981-2008	86.8	0.42	0.87	46.7	2.75	0.43

7	1981-2015	59.0	0.78	0.56	37.5	3.48	0.33
	1981-2008	86.4	0.43	0.86	44.7	2.80	0.41
9	1981-2015	56.2	0.80	0.54	32.5	3.62	0.27
	1981-2008	84.2	0.46	0.84	40.8	2.90	0.36
11	1981-2015	52.5	0.84	0.49	31.1	3.66	0.23
	1981-2008	84.4	0.46	0.84	48.2	2.71	0.44

(N denotes the number of sample removed in the cross-validation regressions; only the odd numbers of N were listed for short)

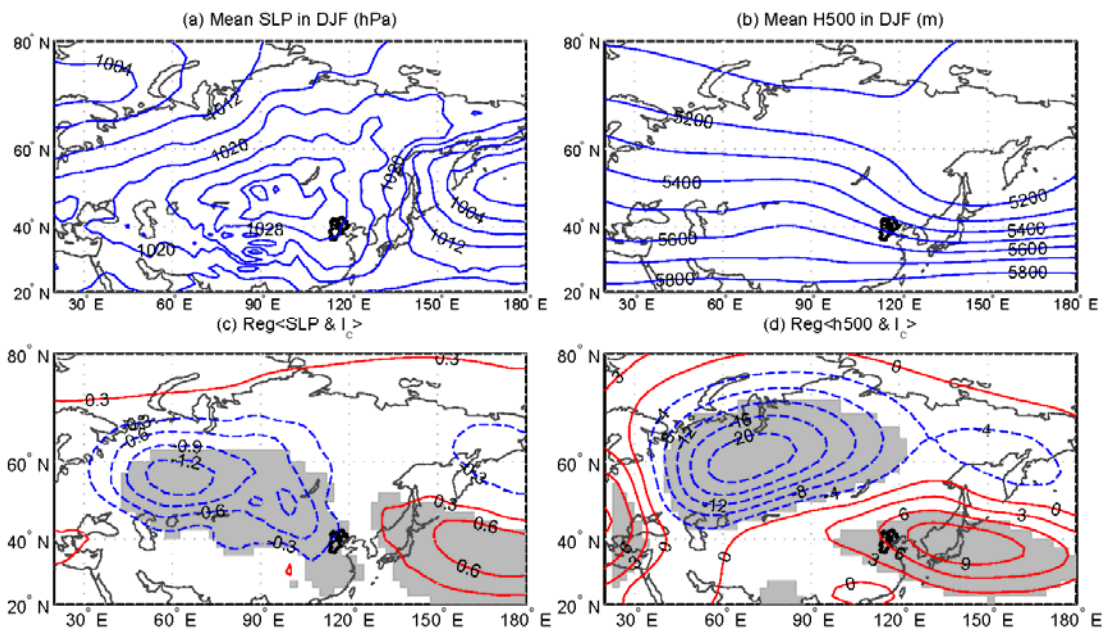
3.4 Possible mechanism of the circulations related to the winter haze pollutions

In order to explore the possible mechanism and role of the investigated circulation indices on the winter visibility and number of hazy days in the BTH region, the links between the given large-scale atmospheric circulations and the local meteorological conditions, which have close relations with the haze pollutions, were examined. For simplicity, a comprehensive index labeled as I_c was synthesized from the six individual circulation indices (I_1 to I_6) by applying a PCA method, namely the first principal component (PC1). The high values of the explained variance (64.4% in PC1) indicated that the comprehensive index of I_c roughly reflect the integrated features of all the six indices. Thus, we used the I_c instead of the six individual indices in the following analysis. Generally, the positive (negative) I_c indicate the lower (higher) visibility and more (less) hazy days in the BTH region in winter.

First we examined the links between the I_c and the meteorological fields of SLP and H500 respectively. Based on the NCEP/NCAR reanalysis data, Figure 6(a) and (b) present the climatological mean of SLP and H500 in winter averaged from 1981 to 2010, respectively. The changes of SLP and H500 in winter in association with a one-standard-deviation positive I_c during the winters 1981 to 2015 are shown in Figure 6(c) and (d), respectively. In the climatological mean fields, the BTH region were located in the trough of East Asian trough at the middle troposphere and in the ridge of Siberian-Mongolia high in SLP field, which indicate the northerly dominated the BTH region in winter. The regression maps show that the SLP decreased in the Siberian-Mongolia high areas and increased in the western Pacific in SLP and the geopotential height decreased in the most areas of Siberia and increased in the northern China to western Pacific. These patterns suggest that both the East Asian trough and Siberian high weaken with increasing I_c , that further implies that the winter cold air activity will be weaken and then lead to an anomalous steady atmospheric conditions in BTH and its adjacent areas

368 in winter. Namely, the less strong Siberian high and East Asian trough and associated
 369 northerly winds in the low and middle troposphere will lead to a severe haze pollution
 370 (lower visibility and more hazy days) due to the favorable meteorological conditions
 371 for the accumulation and chemical reaction of pollutants. Anyway, we wonder whether
 372 it is true as we speculated. We further examined the links between the comprehensive
 373 index of I_c and the local meteorological conditions which play direct roles in the
 374 formation of haze pollutions, including the wind fields (Figure 7), relative humidity
 375 (Figure 8) and vertical velocity (Figure 9) at the lowest troposphere (averaged from
 376 1000 hPa to 900 hPa with an interval of 25 hPa) and the boundary layer height (Figure
 377 10) based on the ERA-Interim reanalysis data.

378
 379



380

381 Figure 6 The climatological mean fields of SLP (a) and H500 (b) averaged in winter 1981 to 2010,
 382 and the spatial distribution of the regression coefficients of SLP (c) and H500 (d) upon the I_c over
 383 the period 1981 to 2015 (Area significant at the 0.05 level are shaded)

384

385 Figure 7(a) displays the climatological mean wind field averaged from 1000 to 900
 386 hPa over the winter 1981 to 2010. At lower level, the northwesterly winds dominated
 387 the BTH, and the wind speed in Beijing, Tianjin and north of Hebei province was larger
 388 than that in the south of Hebei province. Figure 7(b) shows the composite (positive I_c
 389 winters minus negative I_c winters) wind field averaged from 1000 to 900 hPa over the
 390 winter 1981 to 2015. In the composite wind field, the anomalous southeasterly winds
 391 dominated the BTH region instead of the northwesterly in the climatological mean wind

392 field, indicating the weakening of the northwesterly significantly over BTH and its
393 neighboring areas when I_c increased. Previous studies (Zhang et al., 2015) demonstrated
394 the decreasing of wind speed is not conducive to the diffusion of air pollutants and
395 easily lead to haze pollutions in Beijing. It may be true for the whole BTH region. Thus,
396 the increasing of I_c will lead to a decrease in the visibility and increase in the number
397 of hazy days in winter over the BTH region.

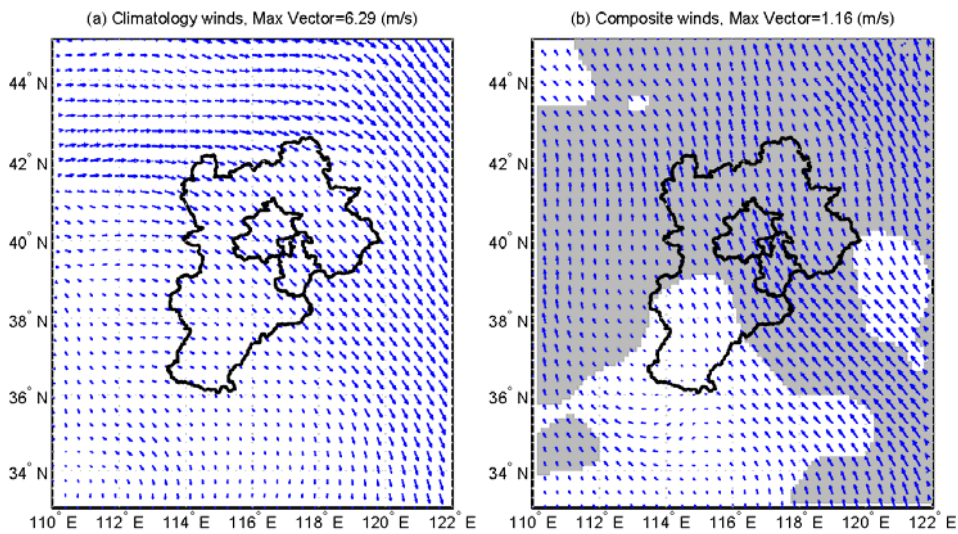
398 Same as Figure 7, Figure 8(a) and (b) present the climatology and composite
399 relative humidity averaged from the lowest troposphere respectively. In the composite
400 map, all the areas of BTH are covered by the positive values and most of them are
401 significant at the 0.05 level. They indicate that the winter relative humidity was
402 anomalous higher in the positive I_c years than that in the negative I_c years. As pointed
403 in the Introduction, a high relative humidity is one of the important reasons for visibility
404 degradation. This is because that the high relative humidity is favorable for the accumulation and
405 hygroscopic growth of pollutants, which can strengthen the light scattering and absorption by
406 atmospheric particles and gases and then cause the visibility degradation directly (Baumer et al.,
407 2008; Zhang et al., 2015). Thus a positive I_c imply that a decreasing of visibility
408 accompanied by the increasing number of hazy days may occur in the winter over BTH
409 region. Figure 9(a) and (b) present the climatology and composite vertical speeds
410 averaged from the lowest troposphere respectively. The positive (negative) values of
411 vertical speed in unit of Pa/s denote sinking (ascending) motion. The climatological
412 vertical speeds show that the downward air motions dominated the BTH region in the
413 winter. In the composite vertical speed field, the most areas of BTH were covered by
414 the significantly negative values, which suggested a less vertical exchanges of air
415 occurred in this areas in the positive I_c winters. In other words, the increased I_c may
416 result in a weaker vertical convection and forcing the lowest troposphere more stable.
417 It's easy to understand the anomalous stabilization will lead to much haze pollutions.
418 Moreover, a similar result can be found in the planetary boundary layer height, which
419 was reduced significantly in the most of BTH and its adjacent areas in the positive I_c
420 winters (Figure 10). The decreased boundary layer height will depress the air pollutants
421 into a narrower air column in a certain area and then lead to an increasing of the
422 pollutants concentration. Thus, a winter with the lower visibility and more hazy days in
423 the BTH region would be expected in the case of the lower boundary layer height
424 caused by the anomalously high I_c .

425 In view of the responses of the local surface winds, relative humidity, vertical
426 motion and boundary layer to the comprehensive index of I_c mentioned above, the close

427 relationships between the winter mean visibility and number of hazy days over BTH
 428 region and the given six atmospheric circulations are generally feasible in the physical
 429 mechanism. It is reasonable and reliable to estimate the winter haze pollutions in the
 430 BTH region based on the seasonal forecast fields derived from climate simulation. Thus
 431 it will be helpful to provide scientific references for the governmental decisions in
 432 advance about the reducing or controlling of pollutants emission to deal with the
 433 probably severe haze pollutions in the BTH region.

434

435

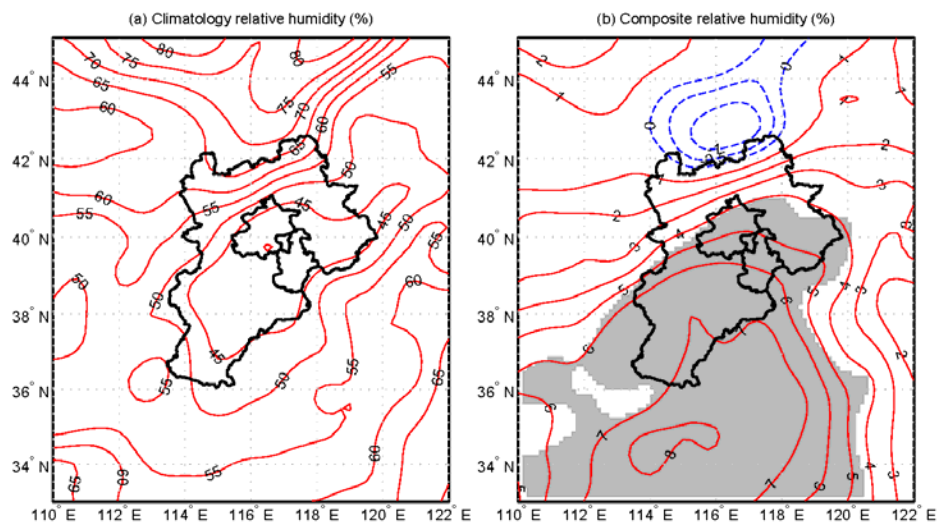


436

437 Figure 7 The climatological mean (a) and the composite (b) wind fields averaged from 1000 to 900
 438 hPa (Area significant at the 0.05 level are shaded)

439

440



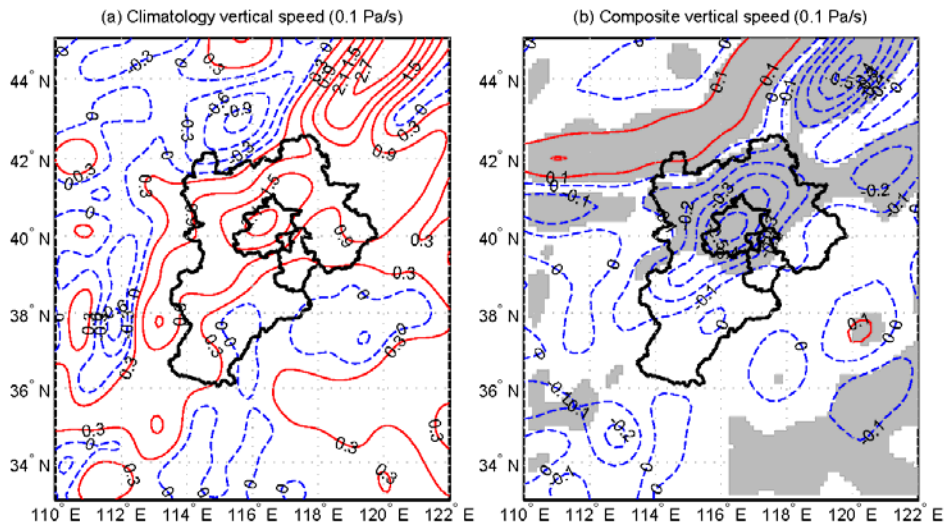
441

442

443

Figure 8 Same as Figure 7, but for relative humidity

444



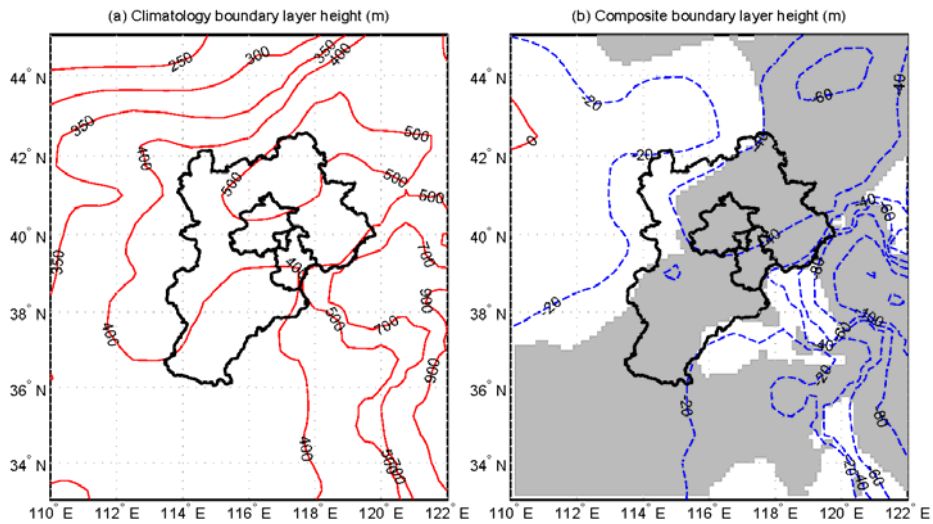
445

446

Figure 9 Same as Figure 7, but for vertical speed

447

448



449

450

Figure 10 The climatological mean (a) and the composite (b) boundary layer height

451

(Area significant at the 0.05 level are shaded)

452

453 4 Conclusions

454

Using the daily visibility and number of hazy days recorded in the 19
455 meteorological stations and the NCEP/NCAR and ERA-Interim reanalysis data, the
456 evolution of the winter haze pollutions in the BTH region since 1981 and their possible
457 relations to atmospheric circulations were examined in this study.

458

The results showed that the winter mean visibility has a significant negative
459 correlation with the number of hazy days and both of them show distinctly inter-annual

460 variability during the entire period 1981 to 2015. The correlation coefficients between
461 the winter haze pollutions (the visibility and number of hazy days) and the most
462 common atmospheric circulations over the mid-high latitude of northern hemisphere
463 were re-examined. Results showed that the relations between the haze pollutions in
464 BTH and the winter AO, NAO and PNA were very weak, but they correlated
465 significantly with EU, WP and SBH. Furthermore, the six new indices (I_1 to I_6) derived
466 from the key areas in the fields of SLP, U&V850, H500, U200 and T200 were closely
467 related to the winter haze pollutions in BTH. We can estimate the visibility and number
468 of hazy days by using the six indices and the fitting and the leave-N-out cross-validation
469 methods, respectively. In general, the high level of the estimation statistics suggested
470 the winter haze pollutions in BTH can be estimated or predicted in a reasonable degree
471 based on the optimized atmospheric circulation indices. However, we also noted that
472 the statistic estimation models for the visibility and number of hazy days may be
473 influenced in part by a prominent change of the pollutants emission artificially. Thus, it
474 is valuable and significant for government decision-making departments to take actions
475 in advance in dealing with the probably severe haze pollutions in BTH indicated by the
476 circulation conditions, such as to control the pollutants discharge.

477 In order to investigate the link processes between the haze pollutions and the given
478 atmospheric circulations more simply, a comprehensive index (I_c) was synthesized from
479 the six individual circulation indices by applying a PCA method. The winter I_c increase
480 appear to cause a shallowing of the East Asian trough at the middle troposphere and a
481 weakening of the Siberian high pressure field at sea level, and then accompanied by a
482 reduction (increase) of horizontal advection and vertical convection (relative humidity)
483 in the lowest troposphere and a reduced boundary layer height in BTH and its
484 neighboring areas, which are not conducive to the spread and elimination of air
485 pollutants but favor the formation of haze pollutions in BTH winter. In short, the
486 reasonable link processes and the stable statistic relationships suggested that the
487 atmospheric circulation indices can be used to predict or evaluate generally the haze
488 pollutions in BTH winter to some extent.

489

490 **Acknowledgments**

491 This study was supported by Beijing Natural Science Foundation (Grant no. 8152019), the National
492 Key Technologies R & D Program of China (Grant no. 2014BAC23B01 and 2014BAC23B00) and
493 Project PE16010 of the Korea Polar Research Institute. X. Zhang acknowledges the financial
494 support from the Project Z141100001014013 of Beijing Municipal Science & Technology

495 Commission. D. Gong was supported by the National Natural Science Foundation of China (Grant
496 No. 41321001).

497 **Reference:**

498 An, X., Zhu, T., Wang, Z., et al.: A modeling analysis of a heavy air pollution episode
499 occurred in Beijing, *Atmos. Chem. Phys.* 7, 3103–3114, 2007.

500 Baddock, M. C., Strong, C. L., Leys, J. F., Heidenreich, S. K., Tews, E. K., McTainsh,
501 G. H.: A visibility and total suspended dust relationship, *Atmos. Environ.*, 89, 329–
502 336, 2014.

503 Baumer, D., Vogel, B., Versick, S., Rinke, R., Mohler, O., Schnaiter, M.: Relationship
504 of visibility, aerosol optical thickness and aerosol size distribution in an ageing air
505 mass over South-West Germany, *Atmos. Environ.*, 42, 989–998, 2008.

506 Chan, C. K., Yao, X.: Air pollution in mega cities in China, *Atmos. Environ.*, 42, 1–42,
507 2008.

508 Chang, D., Song, Y., Liu, B.: Visibility trends in six megacities in China 1973–2007,
509 *Atmos. Res.*, 94, 161–167, 2009.

510 Chen, Y., Zhao, C. S., Zhang, Q., Deng, Z. Z., Huang, M. Y., Ma, X. C.: Aircraft study
511 of mountain chimney effect of Beijing, China. *J. Geophys. Res.* 114 (D8), D08306.
512 doi:10.1029/2008JD010610, 2009.

513 Dee, D. P., Uppala, S. M., Simmons, A. J., Berrisford, P., Poli, P., Kobayashi, S.,
514 Andrae, U., Balmaseda, M. A., Balsamo, G., Bauer, P., Bechtold, P., Beljaars, A. C.
515 M., Berg, L., Bidlot, J., Bormann, N., Delsol, C., Dragani, R., Fuentes, M., Geer, A.
516 J., Haimberger, L., Healy, S. B., Hersbach, H., Hólm, E. V., Isaksen, L., Kållberg, P.,
517 Köhler, M., Matricardi, M., McNally, A. P., Monge-Sanz, B. M., Morcrette, J. J.,
518 Park, B. K., Peubey, C., Rosnay, P., Tavolato, C., Thépaut, J. N., Vitart, F.: The ERA-
519 Interim reanalysis: Configuration and performance of the data assimilation system,
520 *Q. J. R. Meteorol. Soc.*, 137, 553–597, 2011.

521 Deng, J. J., Xing, Z. Y., Zhuang, B. L., Du, K.: Comparative study on long-term
522 visibility trend and its affecting factors on both sides of the Taiwan Strait, *Atmos.*
523 *Res.*, 143, 266–278, 2014.

524 Ding, Y. H.: A statistical study of winter monsoons in East Asia, *J. Trop. Meteor.*, 6(2),
525 119–128, 1990 (in Chinese).

526 Feng, J. L., Hu, M., Chan, C. K., Lau, P. S., Fang, M., He, L. Y., Tang, X. Y.: A
527 comparative study of the organic matter in PM_{2.5} from three Chinese megacities in
528 three different climatic zones, *Atmos. Environ.* 40, 3983–3994, 2006.

529 Fritts, H. C.: *Tree-Rings and Climate*, Academic Press, London, 567pp, 1976.

530 Gao, Y., Liu, X., Zhao, C., et al.: Emission controls versus meteorological conditions
531 in determining aerosol concentrations in Beijing during the 2008 Olympic Games,
532 *Atmos. Chem. Phys.* 11, 12437–12451, 2011.

533 Gong, D. Y., Ho, C.H.: Siberian High and climate change over middle to high latitude
534 Asia, *Theor. Appl. Climatol.*, 72, 1–9, 2002.

535 Gong, D. Y., Luterbacher, J.: Variability of the low-level cross-equatorial jet of the
536 western Indian Ocean since 1660 as derived from coral proxies. *Geophys. Res. Lett.*,
537 35, L01705, doi:1029/2007GL032409, 2008.

538 Gong, D. Y., Zhu, J. H., Wang, S. H.: The influence of Siberian High on large-scale
539 climate over continental Asia, *Plateau Meteor.*, 21(1), 8–14, 2002 (in Chinese).

540 Kalnay, E., Kanamitsu, M., Kistler, R., Collins, W., Deaven, D., Gandin, L., Iredell, M.,
541 Saha, S., White, G., Woollen, J., Zhu, Y., Leetmaa, A., Reynolds, B., Chelliah, M.,
542 Ebisuzaki, W., Higgins, W., Janowiak, J., Mo, K. C., Ropelewski, C., Wang, J., Jenne,
543 R., Joseph, D.: The NCEP/NCAR 40-year reanalysis project, *Bull. Amer. Meteor.*
544 *Soc.*, 77, 437–471, 1996.

545 Kang, H. Q., Zhu, B., Su, J. F., Wang, H. L., Zhang, Q. C., Wang, F.: Analysis of a long-
546 lasting haze episode in Nanjing, China, *Atmos. Res.*, 120, 78–87, 2013.

547 Li, Y., Lu, R. Y., He, J. H.: Several climate factors influencing the winter temperature
548 over China, *Chinese J. Atmos. Sci.*, 31(3), 505–514, 2007 (in Chinese).

549 Liu, S. H., Liu, Z. X., Li, J., Wang, Y. C., Ma, Y. J., Sheng, L., Liu, H.P., Liang, F. M.,
550 Xin, G. J., Wang, J. H.: Numerical simulation for the coupling effect of local
551 atmospheric circulations over the area of Beijing, Tianjin and Hebei Province, *Sci.*
552 *China Ser. D-Earth*, 52 (3), 382–392, 2009.

553 Lo, J. C. F., Lau, A. K. H., Fung, J. C. H., Chen, F.: Investigation of enhanced cross-
554 city transport and trapping of air pollutants by coastal and urban land-sea breeze
555 circulations. *J. Geophys. Res.* 111 (D14), D14104. doi: 10.1029/2005JD006837,
556 2006.

557 Miao, Y. C., Liu, S. H., Zheng, Y. J., Wang, S., Chen, B. C., Zheng, H., Zhao, J. C.:
558 Numerical study of the effects of local atmospheric circulations on a pollution event
559 over Beijing–Tianjin–Hebei, China, *J. Environ. Sci.*, 30, 9–20, 2015.

560 Sabetghadam, S., Farhang, A. G., Golestani, Y.: Visibility trends in Tehran during
561 1958-2008, *Atmos. Environ.* 62, 512–520, 2012.

562 Schichtel, B. A., Husar, R. B., Falke, S. R., Wilson, W. E.: Haze trends over the United
563 States 1980-1995, *Atmos. Environ.*, 35(30), 5205–5210, 2001.

564 Streets, D. G., Fu, J. H. S., Jang, C. J., Hao, J., He, K. B., Tang, X. Y., Zhang, Y. H.,
565 Wang, Z. F., Li, Z. P., Zhang, Q., Wang, L. T., Wang, B. Y., Yu, C.: Air quality

566 during the 2008 Beijing Olympic Games, *Atmos. Environ.*, 41(3), 480–492, 2007.

567 Thompson, D. W., Wallace, J. M.: The arctic oscillation signatures in the wintertime
568 geopotential height and temperature fields, *Geophys. Res. Lett.*, 25(9), 1297–1300,
569 1998.

570 Wallace, J. M., Gutzler, D. S.: Teleconnections in the geopotential height field during
571 the Northern Hemisphere winter, *Mon. Wea. Rev.*, 109, 784–812, 1981.

572 Wang, H. J., Chen, H. P., Liu, J. P.: Arctic Sea Ice Decline Intensified Haze Pollution
573 in Eastern China, *Atmos. Oceanic Sci. Lett.*, 8(1), 1–9, 2015.

574 Wang, T., Nie, W., Gao, J., Xue, L. K., Gao, X. M., Wang, X. F., Qiu, J., Poon, C. N.,
575 Meinardi, S., Blake, D., Wang, S. L., Ding, A. J., Chai, F. H., Zhang, Q. Z., and
576 Wang, W. X.: Air quality during the 2008 Beijing Olympics: secondary pollutants
577 and regional impact, *Atmos. Chem. Phys.*, 10, 7603–7615, 2010.

578 Wang, Y., Hao, J., McElroy, M. B., Munger, J. W., Ma, H., Chen, D., and Nielsen, C.
579 P.: Ozone air quality during the 2008 Beijing Olympics: effectiveness of emission
580 restrictions, *Atmos. Chem. Phys.*, 9, 5237–5251, 2009.

581 Wang, Y. S., Yao, L., Liu, Z. R., Ji, D. S., Wang, L. L., Zhang, J. K.: Formation of haze
582 pollution in Beijing-Tianjin-Hebei region and their control strategies, *Chin. Sci. Bull.*,
583 28 (3), 353–363, 2013 (in Chinese).

584 Wen, C. C., Yeh, H. H.: Comparative influences of airborne pollutants and
585 meteorological parameters on atmospheric visibility and turbidity, *Atmos. Res.*,
586 96(4), 496–509, 2010.

587 Wu, D., Chen, H. Z., Wu, M., Liao, B. T., Wang, Y. C., Liao, X. N., Zhang, X. L.,
588 Quan, J. N., Liu, W. D., Gu, Y., Zhao, X. J., Meng, J. P., Sun, D.: Comparison of
589 three statistical methods on calculating hazy days-taking areas around the capital for
590 example, *China Environ. Sci.*, 34(3), 545–554, 2014 (in Chinese).

591 Xu, W. Z., Chen, H., Li, D. H., Zhao, F. S., Yang, Y.: A case study of aerosol
592 characteristics during a haze episode over Beijing, *Procedia. Environ. Sci.* 18, 404–
593 411, 2013.

594 Zhang, Q. H., Zhang, J. P., Xue, H. W.: The challenge of improving visibility in Beijing,
595 *Atmos. Chem. Phys.* 10, 7821–7827, 2010.

596 Zhang, Q., Quan, J. L., Tie, X. X., Li, X., Liu, Q, Gao, Y., Zhao, D. L.: Effects of
597 meteorology and secondary particle formation on visibility during heavy haze events
598 in Beijing, China, *Sci. Total Environ.*, 502, 578–584, 2015.

599 Zhang, X. L., Huang, Y. B., Zhu, W. Y., Rao, R. Z.: Aerosol characteristics during
600 summer haze episodes from different source regions over the coast city of North
601 China Plain, *J. Quant. Spectrosc. Radiat. Transf.* 122, 180–193, 2013.

602 Zhang, Z. Y., Gong, D. Y., He, X. Z., Lei, Y. N., and Feng, S. H.: Statistical reconstruction of
603 Antarctic Oscillation index based on multi-proxies, *Atmos. Oceanic Sci. Lett.*, 3(5),
604 283–287, 2010.

605 Zhang, Z. Y., Gong, D. Y., Hu, M., Guo, D., He, X. Z., and Lei, Y. N.: Anomalous winter
606 temperature and precipitation events in southern China, *J. Geogra. Sci.*, 19(4), 471–
607 488, 2009.

608 Zhang, Z. Y., Zhang, X. L., Gong, D. Y., Quan, W. J., Zhao, X. J., Ma, Z. Q., and Kim, S. J.: Evolution
609 of surface O₃ and PM_{2.5} concentrations and their relationships with meteorological
610 conditions over the last decade in Beijing, *Atmos. Environ.*, 108, 67–75, 2015.

611 Zhao, X. J., Zhang, X. L., Xu, X. F., Xu, J., Meng, W., and Pu, W. W.: Seasonal and diurnal
612 variations of ambient PM_{2.5} concentration in urban and rural environments in Beijing,
613 *Atmos. Environ.* 43, 2893–2900, 2009.

614 Zhao, X. J., Zhao, P. S., Xu, J., Meng, W., Pu, W. W., Dong, F., He, D., and Shi, Q. F.: Analysis of a
615 winter regional haze event and its formation mechanism in the North China Plain,
616 *Atmos. Chem. Phys.*, 13, 5685–5696, 2013.

617

618